International Journal of Pharmaceutics 393 (2010) 41–47

Contents lists available at ScienceDirect

International Journal of Pharmaceutics

journal homepage: www.elsevier.com/locate/ijpharm

Solventless visible light-curable coating: II. Drug release, mechanical strength and photostability

Sagarika Bose[a,1], Robin H. Bogner[a,b,*]

[a] Department of Pharmaceutical Sciences, School of Pharmacy, University of Connecticut, 69 North Eagleville Road, Storrs, Connecticut 06269, United States
[b] Institute of Material Science, University of Connecticut, 97 North Eagleville Road, Storrs, Connecticut 06269, United States

ARTICLE INFO

Article history:
Received 25 November 2009
Received in revised form 22 March 2010
Accepted 27 March 2010
Available online 3 April 2010

Keywords:
Coating
Pellets
Percolation
Simulation
Controlled release
Photostability

ABSTRACT

Solventless photocurable film coating was used to obtain modified release coatings. Different pore-forming agents were used to achieve immediate and sustained release of a blue dye contained in the coated pellets (non-pareil beads). A super-disintegrant, sodium starch glycolate, was used to obtain immediate release. When incorporated in the coating, this pore-former swelled and yielded large pores that demonstrated quick release of the marker dye while leaving behind the scaffold provided by the photocured polymer. Simple pore-formers (lactose and sodium chloride) dissolved away without swelling and provided a more sustained release profile. Release can be modified with the choice of material, number of layers and thickness of the coating. When release of sodium chloride and release of marker dye were simultaneously monitored, it was observed that at least 40–50% of the sodium chloride that was incorporated in the coating released before the dye was released through the coating showing that pore-formation preceded the release of the marker dye. The coupling factor between dye release and pore-formation was found to be dependent on the ratio of amount of solid pore-forming agent and volume of liquid monomer (S/L) of the coating. Also, studies demonstrate that the coating is photostable and can withstand handling stress.

1. Introduction

Film coating is generally accomplished by spraying polymers dissolved in solvents onto a cascading bed of tablets. The disadvantages associated with the use of solvents (both aqueous and organic) can be overcome by the use of solventless coating technologies (Bose and Bogner, 2007a). Photocurable coating can be formed at room temperature or below (Yang, 1993a,b) by a polymerization reaction involving a free radical, cationic or anionic mechanism depending on the functional groups of the liquid prepolymers or monomers and initiators or catalyst to form a solid film (Kutal et al., 1991). Photocuring systems generally include of three major components: light source, specially functionalized liquid prepolymers or monomers and an initiator (Pappas, 1985). Oxygen acts a scavenger molecule if present in the system, thereby slowing down and/or reducing the extent of curing in some acrylate-functionalized silicone systems by quenching excited states and scavenging free radicals from the initiator and the growing polymer network (Decker et al., 1980). Thus, photocurable systems are usually purged with nitrogen to reduce this complication.

Photocuring has wide commercial application in dental and medical fields (Kurze, 1994). Composite dental fillings (Lovell et al., 2001; Tanoue et al., 1998), preventive treatment for caries (Wilder et al., 1999, 1983), assembly of medical devices (Burger, 2000), and wound dressing (Lee et al., 1992; Szycher et al., 1985, 1986a,b; Trotter, 2002) are a few examples of its use. Photocuring for film coating of pharmaceuticals is still in the early investigational phase. A UV-curable film coating system consisting of derivatized silicone prepolymers along with a photoinitiator, benzoin methyl ether, was used to coat pellets (non-pareil beads) (Wang and Bogner, 1995). Free-radical polymerization of the functionalized liquid prepolymers resulted in transition from a liquid prepolymer film to solid coating with sufficient integrity. However, these coatings were impermeable to drug release. Later, pharmaceutically functional photocurable coatings were prepared by incorporating different powdered pore-forming agents to a photocurable silicone-coating matrix. That process involved UV light in order to cure the acrylate-terminated siloxanes (Bose and Bogner, 2006, 2007b). Evaluation of the coating efficiency, uniformity, photostability, mechanical strength, and release characteristics demonstrated the method to be feasible. However, the use of UV light and lack of toxicity data

* Corresponding author at: Department of Pharmaceutical Sciences, School of Pharmacy, University of Connecticut, 69 North Eagleville Road, Storrs, Connecticut 06269, United States. Tel.: +1 860 486 2136; fax: +1 860 486 2076.
E-mail addresses: bosesagarika@gmail.com (S. Bose), robin.bogner@uconn.edu (R.H. Bogner).
[1] Current address: Pfizer Inc, 401 N. Middletown Road, Pearl River, NY 10965, United States. Tel.: +1 860 888 9127.

0378-5173/$ – see front matter © 2010 Elsevier B.V. All rights reserved.
doi:10.1016/j.ijpharm.2010.03.052

on the photocurable siloxane prepolymers may slow implementation in the pharmaceutical industry. Thus an alternative system was found using visible light and photocurable monomers currently used in dental practice, tetraethyleneglycol dimethacrylate (TEGDMA) and bisphenol A-glycidyl methacrylate (Bis-GMA) (Bose and Bogner, 2010). Similar to the photocurable siloxane system, the ratio of pore-formers in the coating to photocurable liquid, type and particle size of the pore-formers, intensity and exposure time of light and concentration of initiator were found to be critical for the processability (Bose and Bogner, 2006, 2010). The UV-curable coating was strong and photostable. It was feasible to obtain immediate as well as sustained release by changing the pore-forming agent in the coating as well as with choice of material, number of layers and thickness of the coating (Bose and Bogner, 2007b). The current work investigates whether similar properties can be obtained from the visible light-curable system.

2. Materials and methods

2.1. Materials

Two photocurable monomers, tetraethyleneglycol dimethacrylate (TEGDMA) and bisphenol A-glycidyl methacrylate (Bis-GMA), were available from Rohm America (Piscataway, NJ) and ESS Tech (Essington, PA), respectively. Camphorquinone (CQ), a photosensitizer, and 2-(dimethylamino) ethyl methacrylate (DMAEMA), a photoinitiator, were obtained from Aldrich (St. Louis, MO). Nonpareil beads (14–18 mesh) containing FD&C #1 as a marker dye were available from Ozone Confectioners (Elmwood Park, NJ). Explotab® (sodium starch glycolate) was available from Penwest Pharmaceutical Co. (Patterson, NY) and used in the particle size range of 45–63 μm. Lactose (spray-dried, grade #315) was obtained from Foremost (Baraboo, WI) and used in the particle size range of 75–106 μm. Sodium chloride was available from Fisher Scientific (Fairlawn, NJ) and used in the particle size range of 75–106 μm. Ac-Di-Sol® (croscarmellose sodium) was obtained from FMC Biopolymer (Newark, DE) and used in the particle size range of 45–63 μm. All materials were stored as advised by the providers.

2.2. Methods

2.2.1. Coating process

Five grams of non-pareil beads (coated with the FD&C #1 dye) were placed in a mini-coating pan consisting of the bottom 9 cm of a 500 ml Erlenmeyer flask in a drum rotating at 18–19 rpm driven by an all-purpose motor (Erweka, Milford, CT). The 7 cm opening of this mini-coating vessel faced out of the open portion of the drum which was tilted 30° from horizontal. This system is very similar to a traditional pan-coating system. A custom built chamber was fitted over the coating pan and continually purged with nitrogen at a rate of 0.5 l/min to reduce the presence of oxygen. Through a small port in the chamber, the monomer liquid consists of 70:30 TEGDMA:Bis-GMA (90% (w/w) and 1:4 CQ:DMAEMA (10% (w/w) was pipetted onto the bed of beads and allowed to distribute for 1 min. These ratios were previously determined to be optimal (Bose and Bogner, 2010). A powdered pore-forming agent (lactose, sodium chloride, Explotab® or Ac-di-sol®) was dusted onto the bed of monomer coated beads within 10–15 s and allowed to distribute for 1 min. Then the system was purged with nitrogen for 3 min to reduce the presence of oxygen. The volumes of monomer liquid (L) and amounts of powdered pore-forming solids (S) used to prepare batches with various S/L ratios found to produce good coating uniformity are listed in Table 1. Coating uniformity was measured by digital image analysis as previously described in detail (Bose and Bogner, 2006).

After incorporating the pore-former and closing the front port, the chamber was purged with nitrogen for an additional 3 min. The beads were exposed to 82500 lux of visible light (Right Touch, Work light, Model # RT-83992, Fountain Valley, CA) through the front quartz panel of the nitrogen-filled chamber for 15 min. The coating procedure was repeated to produce 3–6 layers. All batches were prepared in triplicate.

2.2.2. Release performance

Release of the marker dye FD&C Blue #1, from within the core of the coated beads was determined by placing the weight equivalent to 3 g of uncoated beads in a USP Type II apparatus (Vanderkamp 600, Vankel Industries, Inc., Chatham, NJ) with 250 ml of doubly distilled water at 37 °C stirred at 50 rpm. The release of dye from the coated non-pareils was measured over a 1 h period for immediate release coatings and up to 24 h period for sustained release coatings. Absorbance of the released FD&C #1 was measured at 628 nm in a UV spectrophotometer (Model # 8450A, Hewlett Packard, Palo Alto, CA). The release profiles were assessed by similarity factor (f_2) analysis (Food and Drug Administration, 1997b), where f_2 values greater than 50 (range 50–100) indicated similarity in results (Food and Drug Administration, 1997b).

The pore structure of the coating was evaluated by monitoring the release of sodium chloride (one of the pore-formers) from the coating itself by conductance (Model 34, YSI, Yellow Springs, Ohio) at the same time points (0–12 h) as dye release was measured.

2.2.3. Thickness of the coatings

The average diameter of approximately 200 beads from each batch of coated and uncoated beads were determined using a 5.1 pixel CCD camera and image analysis software (Image-pro®, Media Cybernetics, Silver Spring, MD). The average thickness of the coating from each batch was estimated by subtracting the average diameter of an uncoated batch from that of coated batches of beads and dividing by 2. The mean and standard deviations of these pairwise calculations were reported as average thicknesses of the coating along with their standard deviations.

2.2.4. Mechanical strength of the coating

Six batches of pellets (non-pareil beads) were coated with 6 layers of liquid photocurable monomer consists of 70:30 TEGDMA:Bis-GMA (90% (w/w) and 1:4 CQ:DMAEMA (10% (w/w) and lactose using an S/L ratio of 2.4. Samples from three batches of coated beads, equivalent to 3 g of uncoated beads, were stressed in a friabilator (TA, Erweka GmbH, Heusenstamm, Germany) at 25 rpm for 16 min for the total of 400 revolutions. Unstressed beads from

Table 1
Pore-forming agents and their optimum S/L ratios for optimum process efficiency and coating uniformity (Bose and Bogner, 2010).

Pore-forming agent (particle size range)	Optimum S/L ratio[a] (range studied)	Volume of liquid (μl)[b]	Amount of pore-formers (mg)
Lactose (75–106 μm)	2.4 (1.8–3.0)	500	1200
Sodium chloride (75–106 μm)	3.6 (3.0–4.2)	500	1800
Explotab® (45–63 μm)	3.0 (2.4–3.6)	500	1500

[a] S/L ratio is defined as the ratio of amount of solid pore-forming agent to the volume of monomer. The operational range (in parenthesis) is the range where coating efficiency and uniformity are independent of S/L ratio.
[b] Coating liquid consists of 70:30 TEGDMA:Bis-GMA (90% (w/w) and 1:4 CQ:DMAEMA (10% (w/w).

the same batches as the stressed coated beads were uses as controls. Stressed beads from the friabilator were assessed for any weight loss and then placed in a USP Type II dissolution apparatus with 250 ml of water at 30 °C stirred at 50 rpm and release profiles of stressed and unstressed beads were compared by similarity factor analysis (Food and Drug Administration, 1997b). Samples were withdrawn at intervals and monitored for dye release at 628 nm.

2.2.5. Photostability of the coating

Twenty-one batches of pellets (non-pareil beads) were coated with 6 layers of monomer solution consists of 70:30 TEGDMA:Bis-GMA (90% (w/w) and 1:4 CQ:DMAEMA (10% (w/w) with lactose as pore-forming agent using an S/L ratio of 2.4. A portion of the coated beads (equivalent to 3 g of uncoated beads) from each batch was placed in a light cabinet (CPS+ Suntest, Atlas Materials Testing Technology, Chicago, IL) according to ICH guidelines with one dose of light equivalent to 1.2 million lux hours in 21.8 h with the irradiance of 250 W/m^2 (Food and Drug Administration, 1996, 1997a). Three sets of samples (each set in triplicate) of coated beads were exposed to one, two or three doses of light in closed glass bottles placed on their sides for maximum light exposure (Qorpak® clear glass bottles, 0.5 oz, AP#2101, Fisher Scientific, Springfield, NJ). Control sets consisting of three sets of samples (each set in triplicate) in closed glass bottles covered with aluminum foil were placed in the light cabinet for the equivalent of one, two or three doses of light. One set of samples ($n = 3$) of coated beads was directly exposed to one dose of light in an open glass Petri dish (designated "DE 1X"). The temperature in the light cabinet was maintained at 30 °C with a cooler attached to the instrument. Each exposed coated batch and each control were separately placed in a USP Type II dissolution apparatus with 250 ml of water at 37 °C and a paddle speed of 50 rpm. Samples were withdrawn periodically and evaluated for dye release at 628 nm to determine any differences in coating performance upon light exposure.

2.2.6. Simulation of percolation through the porous coating

A matrix of 110 × 110 × 6 was generated by setting each cell in the matrix to either 1 (i.e., containing pore-former) or 100 (containing undissolvable scaffold polymer matrix) to reflect the volume ratio of pore-former in a coating. This simulation assumes Cartesian coordinates for the coating as a first approximation. The shortest possible path (i.e., minimum number of connected (value = 1) cells) was searched using an algorithm to connect particles between layers in the inner 100 × 100 × 6 matrix to avoid end effects. In one simulation, the algorithm searched 21 possible connections to each cell whereas in an enhanced algorithm, the search was increased to 30 possible ways to connect to the next layer. The cells in the first of 6 layers that were connected to a cell or cells in the 6th layer were considered available pores. The porosity for the purposes of evaluating diffusion through the film was calculated as the fraction of available pores relative to the total number of cells (10,000) in the first layer. For each of those available pores, the minimum path through the 6 layers (generally, 6–12 cells) was calculated. The average path length was divided by 6 to report as the tortuosity of the coating. The variance of the tortuosity was also calculated. It was seen that the enhanced algorithm (i.e., searching 30 vs. 22 connections per cell) resulted in higher porosities and lower tortuosities; the differences were more prominent at lower volume fractions of pore-former, but the results were qualitatively similar in the curve shapes and inflection points.

3. Result and discussion

The ratio of powdered pore-forming solid (S) to photocurable monomer liquid (L) in the coating (the S/L ratio) was found to be a key parameter to obtaining good process efficiency and coating uniformity (Bose and Bogner, 2006). *Coating efficiency and process efficiency* are measures of how much of the polymer and pore-forming agent were effectively incorporated during the process (Bose and Bogner, 2010). The operating range of S/L ratios within which coating efficiency and uniformity were independent of the S/L ratio were previously determined (Table 1) (Bose and Bogner, 2010). At values of S/L ratios below the operating range, the coating uniformity and efficiency declined dramatically. Above the operating range, coating efficiency declined, but less noticeably. For example, using Explotab® as the pore-forming agent, the product quality in terms of process efficiency and coating uniformity was greatest at a solid-to-liquid ratio between 2.4 and 3.6 (with 500 μl of monomer solution and 1200–1800 mg of Explotab® per layer) when particle sizes of Explotab® between 45 and 63 μm were used. Thus, an S/L ratio of 3.0 (the midpoint of 2.4–3.6 range) was selected for the release study with Explotab® in order to ensure the lowest coating variability during release studies. Similarly, the optimum S/L ratio for each pore-former (Table 1) was used for present studies unless otherwise specified. Using these parameters, the release of a marker dye through pores formed by dissolution or swelling of pore-forming agents in the coating was investigated.

3.1. Release studies using simple pore-formers

Lactose was evaluated as a pore-former in coatings of 4, 5 and 6 layers at three S/L ratios. The three S/L ratios, 1.8, 2.4 and 3.0, were within the operating range (Table 1) (Bose and Bogner, 2010). The release profiles of the dye from the cores of each batch of coated beads (equivalent to 3 g of uncoated beads) were assessed in USP Type II dissolution apparatus with 250 ml of doubly distilled water at 37 °C stirred at 50 rpm. At all S/L ratios the release of dye from within the coated beads was significantly lower with each additional layer of coating (Fig. 1A–C). When the profiles were analyzed by similarity factor analysis, the dye release from 6 layer coatings with S/L ratios of 1.8 and 3.0 was greater than from the coatings with S/L ratio 2.4. The 4 and 5 layer coatings showed a significant increase in dye release with increasing S/L ratio (1.8 = 2.4 < 3.0). The difference in release from the coatings prepared with the two low levels of lactose (S/L of 1.8 and 2.4) was primarily due to increasing lag time (2 min for 4 layers to 4 min for 6 layers for S/L 1.8, 2 min for 4 layers to 10 min for 6 layers for S/L 2.4) with an increasing number of layers (Fig. 1A and B). At an S/L ratio of 3.0 (Fig. 1C), there was no appreciable lag time. Rather, the differences in the release profiles between 6 layers and 4 or 5 layers of coating were in release rates (i.e., slopes of the profiles).

Increasing coating thickness generally resulted in the expected decrease in release of the marker dye at 180 min (Fig. 2A). However, unexpectedly, the lower S/L ratio coatings were notably thicker than the higher S/L ratio coatings, and yet resulted in an increase in release rate for lactose-filled coatings. One might have expected that a higher S/L ratio would produce a higher porosity in the coating allowing faster release. In the current work, the S/L ratio is probably offset by the lower coating efficiency (a measure of powder incorporation). The coating efficiency was 80% when the S/L ratio was 1.8 whereas it was lower (68%) at an S/L ratio of 3.0. Thus, all the powder that was introduced in the coating pan was not incorporated into the coating, and did not increase the coating thickness as expected. In the previous siloxane-based coating (Bose and Bogner, 2006), a similar explanation cannot be offered since the coating efficiencies were remarkably independent of S/L ratio (Bose and Bogner, 2007b). Therefore, the observation suggests that within these relatively narrow range of S/L ratios, any difference in porosity of the coating is not significant. The coating efficiency, however, is strongly dependent on S/L ratio. The strong dependence of processing on S/L ratio accompanied by the relative independence of release rate on S/L ratio allows the formulator to

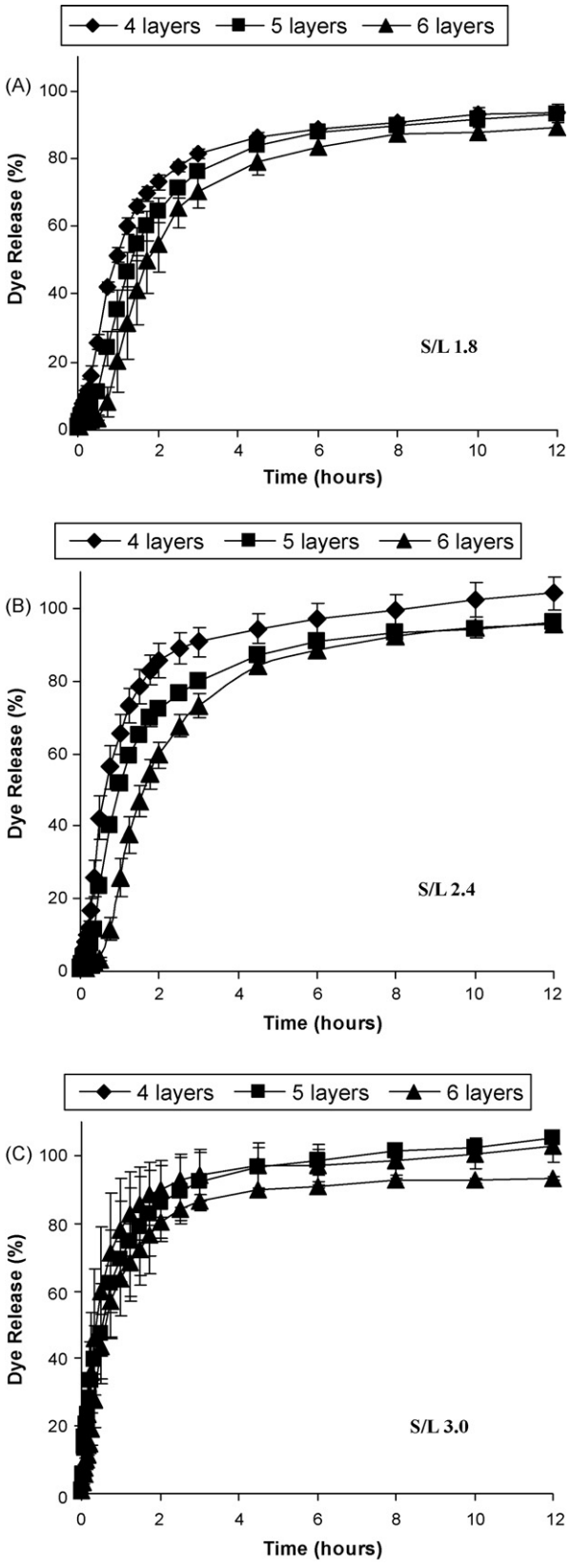

Fig. 1. Dye release from non-pareil beads coated with 4, 5 or 6 layers of coating with liquid monomer consists of 70:30 TEGDMA:Bis-GMA (90% (w/w) and 1:4 CQ:DMAEMA (10% (w/w) and powdered lactose in an amount solid powdered pore-forming agent to volume of liquid monomer ratio (S/L ratio) of (A) 1.8, (B) 2.4, and (C) 3.0.

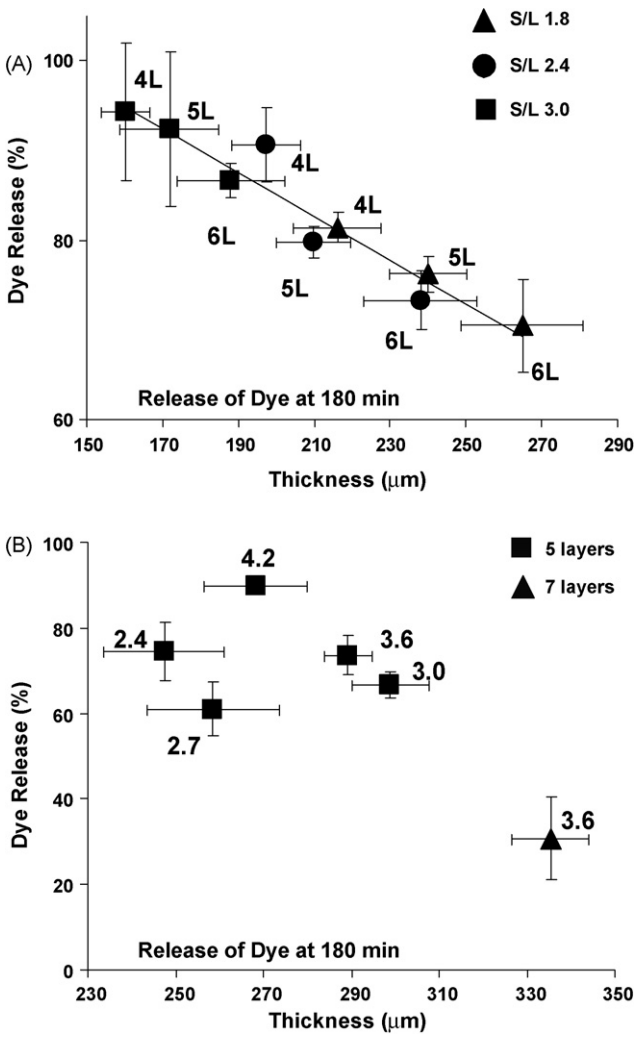

Fig. 2. Dye release at 180 min from non-pareil beads coated with liquid monomer consists of 70:30 TEGDMA:Bis-GMA (90% (w/w) and 1:4 CQ:DMAEMA (10% (w/w) with (A) powdered lactose and (B) powdered sodium chloride as a function of measured coating thickness. Coating thickness was measured using image analysis. S/L ratios are noted next to each point.

independently change the process efficiency (by altering S/L ratio) and release rate (by altering coating thickness).

Sodium chloride was also evaluated as a pore-forming agent for this visible light-curable system. The range of S/L ratios in which sodium chloride provided acceptable coating efficiency (77–84%) along with acceptable uniformity of coating was 3.0–4.2 (Bose and Bogner, 2006). The release of dye was measured from beads coated with 5 layers of coating with S/L ratios of 2.4, 2.7, 3.0, 3.6, and 4.2 using sodium chloride as the pore-former and 7 layers with an S/L ratio of 3.6. Note that the two lowest S/L ratios (2.4 and 2.7) were outside of the optimal range in terms of coating efficiency. There was a general trend toward slower dye release as the S/L ratio increased and a clear decline in dye release with 7 versus 5 layers at an S/L ratio of 3.6 (Fig. 3A). As was described above in the discussion of Fig. 1A and B, the increase in the number of layers resulted in longer time lags for release. The dependence of dye release on thickness of sodium chloride-filled coatings (Fig. 2B) is less clear than was seen for lactose-filled coatings (Fig. 2A). However, when the data from the coatings with the two lowest S/L ratios (those that were outside the optimal range in terms of coating efficiency) (Bose and Bogner, 2006) are neglected, there is a negative correlation of dye release with coating thickness as was seen for lactose-filled coatings (Fig. 2A) and in the UV-curable siloxane-based coating

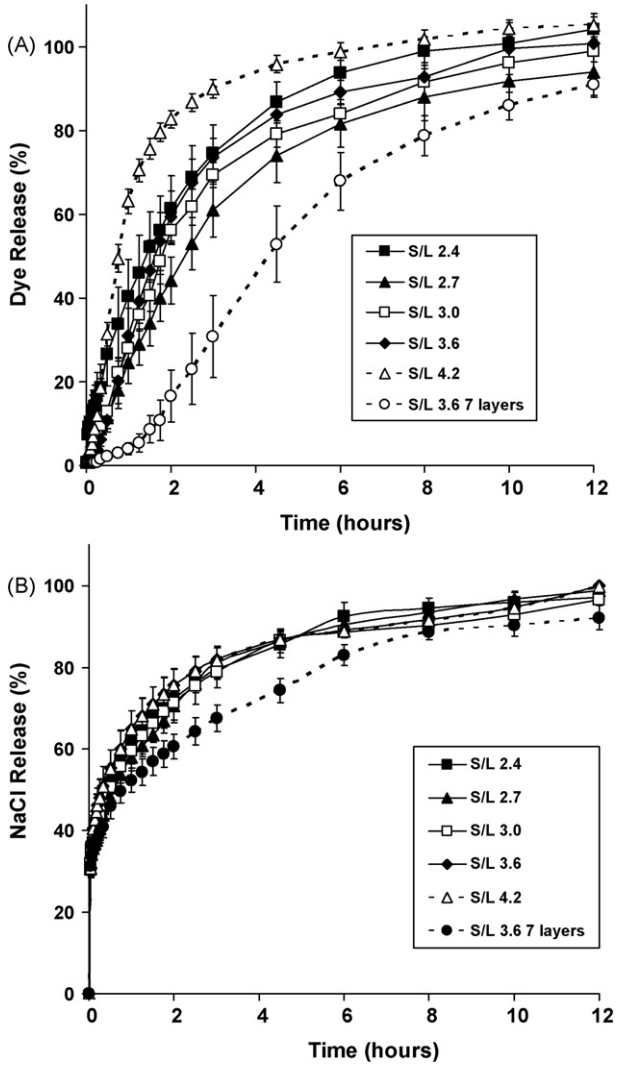

Fig. 3. (A) Dye release (%) and (B) sodium chloride release (%) from the core of non-pareil beads coated with 5 layers (or 7 layers in one case) of coating with liquid monomer consists of 70:30 TEGDMA:Bis-GMA (90% (w/w) and 1:4 CQ:DMAEMA (10% (w/w) and powdered sodium chloride with different S/L ratios.

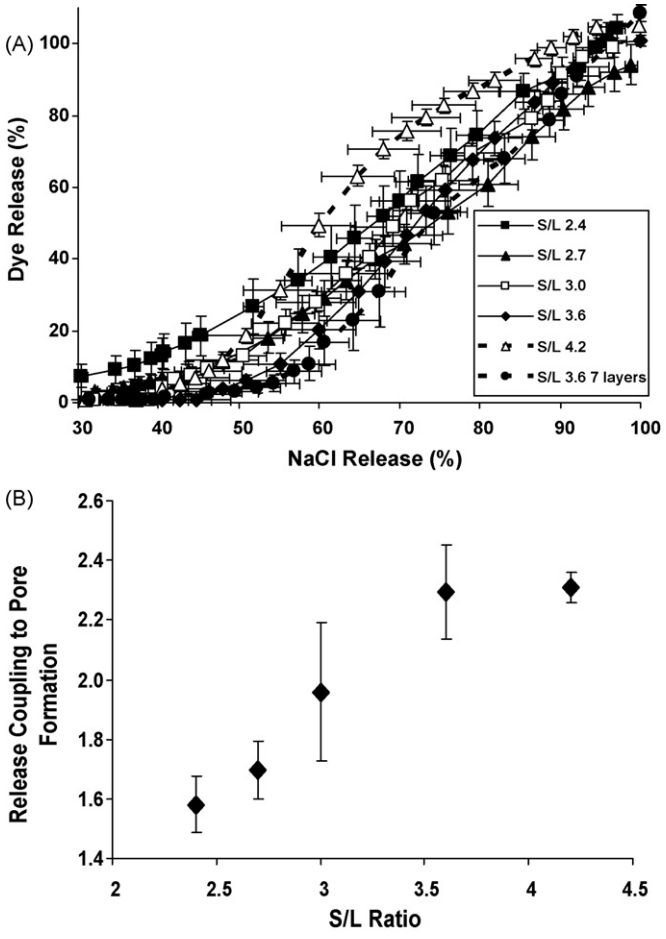

Fig. 4. (A) Dye release from the core of non-pareil beads coated with 5 layers (or 7 layers in one case) of coating with liquid monomer consists of 70:30 TEGDMA:Bis-GMA (90% (w/w) and 1:4 CQ:DMAEMA (10% (w/w) and powdered sodium chloride with different S/L ratios was measured as a function of sodium chloride release from the coating at the same time points. (B) The slope of the linear portion, the release coupling co-efficient, was plotted against S/L ratio.

system (Bose and Bogner, 2006). To understand the release of dye through the coating, release of sodium chloride from the coating itself was monitored. Fig. 3B shows that 25–40% of the incorporated sodium chloride was released immediately. The remainder was released more slowly.

A comparison between the release of sodium chloride from the coating and dye from the bead is shown in Fig. 4A in terms of the fraction of dye and sodium chloride released at the same time point. On average 40–50% of the sodium chloride that was incorporated in the coating released before the dye released through the coating. This is not surprising as pore-formation is a necessary process prior to the release of the marker dye. Eventually, all sodium chloride and dye were released over 24 h. It is observed that there was a remarkably linear portion of Fig. 4A that can be interpreted as a coupling between dye release and pore-formation through sodium chloride release. The slope of that linear portion indicates the degree of coupling between the two profiles. The portion that appeared linear by eye minus the first and last points was used to determine the slope. The R^2 value of each such trend line was greater than 0.99 except for S/L ratio 4.2 (where $R^2 = 0.97$). Fig. 4B shows that the coupling between dye release and pore-formation is dependent on the S/L ratio of the coating. The variance in the tortuosity provides a possible explanation for the shape of Fig. 4B. A computer model for the porosity of the coating was generated. The variance in tortuosity was calculated from the tortuosity values of 50 or more pores. A lower variance in tortuosity means that the paths through the pores are similar, such that the difference in the times to form the first path and the last path upon dissolution of sodium chloride is small. On the other hand, a larger variance in tortuosity would mean that the first path is formed well in advance of the last much more tortuous path, leading to a lower slope in Fig. 4B. The data generated from the computer model (Table 2) show the tortuosity, porosity, and variance in porosity for various coatings as a function of S/L ratio. The porosity increases and the tortuosity decreases as the S/L ratio increases. The apparent diffusion coefficient, which is a function of both porosity, ε, and tortuosity, τ, (i.e., $D\varepsilon/\tau$), increases with S/L ratio, because of both the increase in porosity and the decrease in tortuosity. The doubling of the apparent diffusion coefficient with increasing S/L ratio is too small to account for the differences in the release profiles. However, in the range of S/L ratio from 1.8–4.2, the variance in tortuosity is significant and can account for the change in release coupling seen in Fig. 4B.

In summary, lactose and sodium chloride are useful simple pore-formers. In dissolution media, the powdered pore-forming agents slowly dissolve away and produce pores without swelling. When these pores are connected with each other, they produce channels in the coating through which the dye can be released. Simple

Table 2
Simulated data of tortuosity, porosity, and variance in tortuosity for various coatings as a function of S/L ratio of lactose and sodium chloride.

Solid fraction	Corresponding lactose S/L ratio	Corresponding sodium chloride S/L ratio	Porosity	Tortuosity	Tortuosity variance
0.30	0.7	0.9	0.07	1.56	2.85
0.35	0.8	1.2	0.17	1.52	2.71
0.40	1.0	1.4	0.27	1.48	2.44
0.45	1.3	1.8	0.38	1.43	2.07
0.50	1.5	2.2	0.46	1.36	1.63
0.55	1.9	2.6	0.53	1.31	1.25
0.60	2.3	3.2	0.59	1.25	0.95
0.65	2.9	4.0	0.65	1.21	0.72
0.70	3.6	5.1	0.69	1.17	0.58
0.75	4.6	6.5	0.75	1.14	0.46
0.80	6.2	8.7	0.80	1.11	0.37

pore-formers provide a sustained profile of release of dye from the core.

3.2. Release studies using super-disintegrants to form swollen pores

The dissolution profiles of coatings containing Explotab® as the pore-former were evaluated over 1 h. It was observed that when coatings containing Explotab® came in contact with the dissolution media, no marker dye was released within the first 4 min. Then, the time for 80% release of the dye from the non-pareil was 15 min and 100% of the dye was released in only 20 min (Fig. 5A). The lag time of 4 min was in sharp contrast to the siloxane-based coatings where there was no measurable time lag when Explotab® was used as a pore-former (Bose and Bogner, 2007b). It was observed that the Explotab®-containing coating swelled and broke apart; the result of overcoming the yield point of the strong non-elastic methacrylate material that formed the scaffold containing the pore-former. In the siloxane-based coating system, coating ghosts were collected intact due to the elastic nature of the siloxanes that accommodated the swelling of the Explotab®. Similar to the siloxane-based coating, the immediate release from coatings containing super-disintegrant is in sharp contrast to the slower release of coatings containing the simple pore-formers, lactose and sodium chloride.

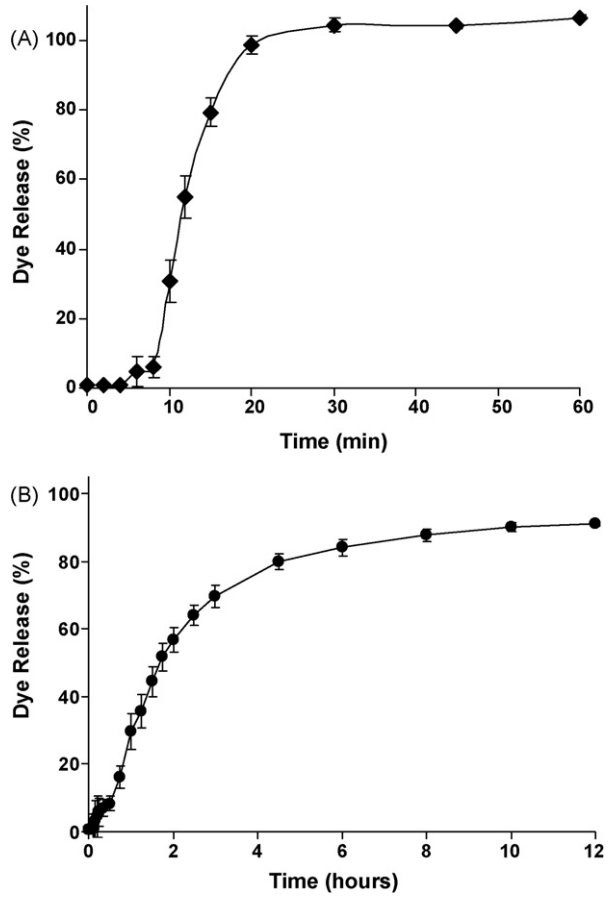

Fig. 5. Dye release from non-pareil beads coated with liquid monomer consists of 70:30 TEGDMA:Bis-GMA (90% (w/w) and 1:4 CQ:DMAEMA (10% (w/w) and (A) powdered Explotab® (4 layers) and for comparison, (B) a combination of 85% beads coated with powdered lactose (6 layers of coating, S/L ratio 2.4) and 15% beads are coated with Explotab® (5 layers of coating, S/L ratio 3.0).

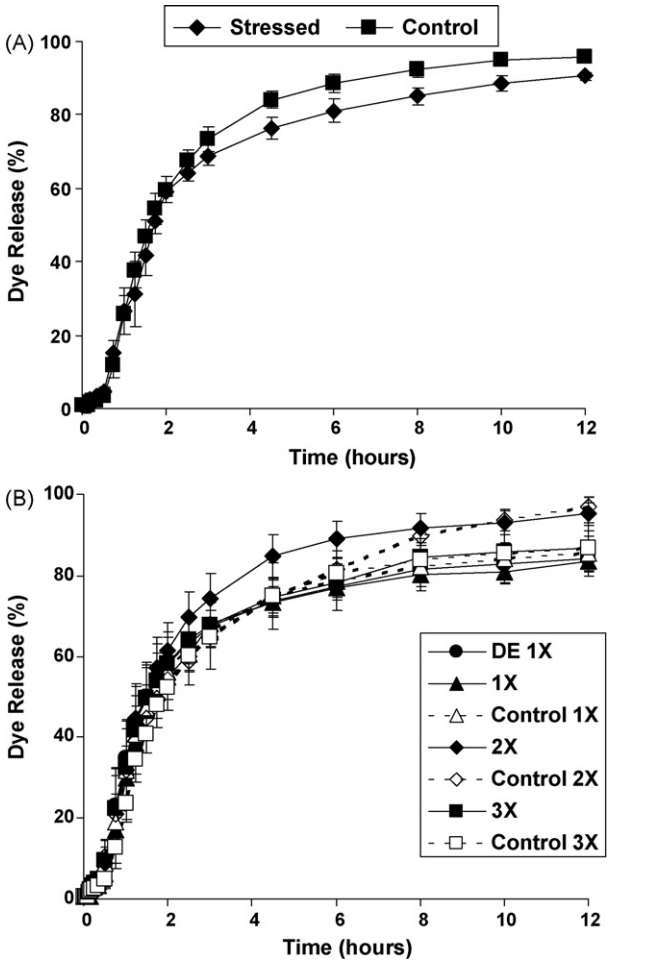

Fig. 6. Non-pareil beads were coated with 6 layers of coating with coating liquid consists of 70:30 TEGDMA:Bis-GMA (90% (w/w) and 1:4 CQ:DMAEMA (10% (w/w) and powdered lactose with S/L ratio of 2.4. (A) One part of the coated beads was stressed with friability test. (B) Coated beads were exposed to 1, 2 or 3 doses of light in a bottle or open glass Petri dish (DE 1X). Release of the blue dye was measured by spectrophotometer for the stressed or exposed and control sets and their release profiles were compared.

In both coating systems, release can be modified with the choice of material, number of layers and thickness of the coating. Release can be further modified as required by mixing fast-releasing and slow-releasing beads. For example, a mixture of 5% beads coated using Explotab® (5 layers of coating) and 95% beads coated using lactose (6 layers of coating) provided a more sustained release profile with no significant time lag (Fig. 5B).

3.3. Mechanical strength and photostability

Friability testing is often used to evaluate the mechanical strength of dosage forms. This handling stress test may cause some defects that are not visually identifiable, but may affect the functioning of the coating. So, release profiles were evaluated before and after the friability test. The pore-forming agent, lactose, produced a sustained release profile with a lag time (Fig. 1C). Thus, if there were significant numbers of defects in the coating due to the stress, a change in the release profile would be expected.

The release profiles from the stressed and the unstressed sets of coated beads showed no significant difference based on similarity factor analysis and t-test ($\alpha = 0.05$) for all time points (Fig. 6A). This result suggests that the coating is strong and can withstand the usual handling stress during manufacturing and shipping.

In the photostability studies, one dose of light is defined as a total of 1.2 million lux hours in 21.8 h with an irradiance of 250 W/m^2 (Food and Drug Administration, 1996, 1997a). This is equivalent to 1 year of exposure to sunlight in Arizona. The release profiles of (1) coated beads exposed to one dose of light in closed glass bottles, (2) coated beads directly exposed to one dose of light in an open glass Petri dish (DE 1X), and (3) their control (coated beads in closed glass bottle and covered with aluminum foil facing all similar conditions but the light exposure) were compared. The release profiles were compared using similarity factor analysis (Food and Drug Administration, 1997b). All samples (fully exposed, exposed in a clear bottle, and unexposed controls) had similar release profiles (Fig. 6B). This result demonstrates that the coating is photostable according to ICH and FDA guidelines.

4. Conclusion

A prototype visible light-curable solventless coating was developed using a monomer and photosensitizer–photoinitiator combination that is safely used in dental practice. It is possible to obtain functional release from this novel solventless photocurable coating technique by including pore-formers in the coating. Lactose and sodium chloride were found to provide more sustained release performance, where Explotab® was an immediate release pore-forming agent. Moreover, this technique provides the flexibility to modify the release by changing the pore-forming material, amount of solid pore-forming agents to the volume of liquid monomer ratio, number of layers of coatings as well as by mixing different coatings made by different pore-forming agents. Finally, studies demonstrate that the coating is photostable (according to ICH guideline) and can withstand handling stress.

Acknowledgements

The authors acknowledge the help of Dr. Sheri Shamblin for assisting with the photostability studies. Financial support for this project was provided by the NSF Center for Pharmaceutical Processing Research (CPPR), now the Dane O. Kildsig CPPR.

References

Bose, S., Bogner, R.H., 2006. Design space for a solventless photocurable pharmaceutical coating. J. Pharm. Innov. 1, 44–53.
Bose, S., Bogner, R.H., 2007a. Solventless pharmaceutical coating processes: a review. Pharm. Dev. Technol. 12, 115–131.
Bose, S., Bogner, R.H., 2007b. Solventless photocurable film coating: evaluation of drug release, mechanical strength and photostability. AAPS PharmSciTech 8, E1–E10.
Bose, S., Bogner, R.H., 2010. Solventless visible light-curable coating. I. Critical formulation and processing factors. Int. J. Pharm..
Burger, P., 2000. UV curing in medical applications. In: Medical Plastics, 2000, Collected Papers of the 14th International Conference, Vienna, Austria, 2.1–2.6.
Decker, C., Fizet, M., Faure, J., 1980. Oxygen effect on UV curing and photodegradation of organic coatings. Org. Coat. Plast. Chem. 42, 710–715.
Food Drug Administration, Center for Drug Evaluation and Research (CDER), 1996. Guidance for Industry: Q1B Photostability Testing of New Drug Substances and Products. Food and Drug Administration, Rockville, MD, pp. 1–14.
Food Drug Administration, Center for Drug Evaluation and Research (CDER), 1997a. Guidelines for the Photostability Testing of New Drug Substances and Products: International Conference on Harmonisation. Food and Drug Administration, Rockville, MD, pp. 27115–27122.
Food Drug Administration, Center for Drug Evaluation and Research (CDER), 1997b. Guidance for Industry: Dissolution Testing of Immediate Release Solid Oral Dosage Forms. Food and Drug Administration, Rockville, MD.
Kurze, U., 1994. Process and apparatus for UV-curing of plastics, Ger. Offen. (Germany), p. 4.
Kutal, C., PA, G., Yang, D.B., 1991. A novel strategy for photoinitiated anionic polymerization. Macromolecules 24, 6872–6873.
Lee, M.S., Gleason, J., Taller, R.A., 1992. Ultraviolet Cured Peelable Film and Method Therefor. Becton, Dickinson and Company, Franklin Lakes, NJ.
Lovell, L.G., Lu, H., Elliott, J.E., Stansbury, J.W., Bowman, C.N., 2001. The effect of cure rate on the mechanical properties of dental resins. Dent. Mater. 17, 504–511.
Pappas, S.P., 1985. UV curing by radical, cationic and concurrent radical-cationic polymerization. Radiat. Phys. Chem. 25, 633–641.
Szycher, M., Battiston, G.C., Vincent, J., Rolfe, J.L., 1985. Advanced UV-curable polyurethanes for wound dressings. In: National SAMPE Symposium and Exhibition, pp. 510–523.
Szycher, M., Dempsey, D.J., Rolfe, J.L., 1986a. Drug dispensing wound dressing, Eur. Pat. Appl., to Thermedics, Inc., USA, p. 26.
Szycher, M., Setterstrom, J.A., Vincent, J.W., Battistone, G., 1986b. Spandra: a sustained release battlefield wound dressing. J. Biomater. Appl. 1, 274–304.
Tanoue, N., Matsumura, H., Atsuta, M., 1998. The influence of ultraviolet radiation intensity on curing depth of photo-activated composite veneering materials. J. Oral Rehabil. 25, 770–775.
Trotter, S., 2002. Backing Material for Plasters and Dressing. Beiersdorf AG, Hamburg, DE.
Wang, J.Z.Y., Bogner, R.H., 1995. Solvent-free film coating using a novel photocurable polymer. Int. J. Pharm. 119, 81–89.
Wilder, A.D.J., May, J.K.N., Bayne, S.C., Taylor, D.F., Leinfelder, K.F., 1999. Seventeen-year clinical study of ultraviolet-cured posterior composite class I and II restorations. J. Esthet. Dent. 11, 135–142.
Wilder, A.D.J., May, J.K.N., Leinfelder, K.F., 1983. Three-year clinical study of UV-cured composite resins in posterior teeth. J. Prosthet. Dent. 50, 26–30.
Yang, D.B., 1993a. Direct kinetic measurements of vinyl polymerization on metal and silicon surfaces using real-time FT-IR spectroscopy. Appl. Spectrosc. 47, 1425–1429.
Yang, D.B., 1993b. Kinetic studies of photopolymerization using real time FT-IR spectroscopy. J. Polym. Sci. A: Polym. Chem. 31, 199–208.